ACSNANO
www.acsnano.org
ARTICLE

Electric-Field-Driven Direct Desulfurization

Bogdana Borca,[*,†,‡,¶] Tomasz Michnowicz,[†,¶] Rémi Pétuya,[§,∇,¶] Marcel Pristl,[†] Verena Schendel,[†,○] Ivan Pentegov,[†] Ulrike Kraft,[†,◆] Hagen Klauk,[†] Peter Wahl,[†,∥] Rico Gutzler,[†] Andrés Arnau,[§,⊥] Uta Schlickum,[*,†] and Klaus Kern[†,#]

[†]Max Planck Institute for Solid State Research, 70569 Stuttgart, Germany
[‡]National Institute of Materials Physics, 077125 Măgurele-Ilfov, Romania
[§]Donostia International Physics Centre, E-20018 Donostia - San Sebastián, Spain
[∥]SUPA, School of Physics and Astronomy, University of St. Andrews, North Haugh, St. Andrews KY16 9SS, United Kingdom
[⊥]Departamento de Física de Materiales UPV/EHU and Material Physics Center (MPC), Centro Mixto CSIC-UPV/EHU, E-20018 Donostia - San Sebastián, Spain
[#]Institut de Physique, École Polytechnique Fédérale de Lausanne (EPFL), CH-1015 Lausanne, Switzerland

Supporting Information

ABSTRACT: **The ability to elucidate the elementary steps of a chemical reaction at the atomic scale is important for the detailed understanding of the processes involved, which is key to uncover avenues for improved reaction paths. Here, we track the chemical pathway of an irreversible direct desulfurization reaction of tetracenothiophene adsorbed on the Cu(111) closed-packed surface at the submolecular level. Using the precise control of the tip position in a scanning tunneling microscope and the electric field applied across the tunnel junction, the two carbon−sulfur bonds of a thiophene unit are successively cleaved. Comparison of spatially mapped molecular states close to the Fermi level of the metallic substrate acquired at each reaction step with density functional theory calculations reveals the two elementary steps of this reaction mechanism. The first reaction step is activated by an electric field larger than 2 V nm^{-1}, practically in absence of tunneling electrons, opening the thiophene ring and leading to a transient intermediate. Subsequently, at the same threshold electric field and with simultaneous injection of electrons into the molecule, the exergonic detachment of the sulfur atom is triggered. Thus, a stable molecule with a bifurcated end is obtained, which is covalently bound to the metallic surface. The sulfur atom is expelled from the vicinity of the molecule.**

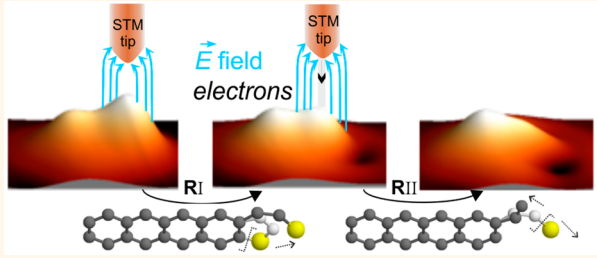

KEYWORDS: *STM, DFT, tetracenothiophene, desulfurization, electric field, single molecules*

Chemical reactions implying the dissociation of carbon−sulfur bonds are fundamental for understanding the carbon and sulfur cycles in nature.[1−3] Moreover, methods for removing the sulfur atoms from organic molecules, the desulfurization reactions, are of industrial significance in processes aimed at cleaning natural fuels.[4] A popular method is based on the use of catalysts to diminish the activation energy of the reaction.[5] Indeed, when released, sulfur compounds may have a detrimental effect on the natural environment.[6] A clear understanding of the mechanism of the reaction by local control down to the submolecular level may help to identify more efficient reaction paths.

Scanning tunneling microscopy (STM) constitutes an adequate tool to trigger and analyze chemical reactions with atomic precision. The formation,[7−10] scission,[11−17] or deformation of chemical bonds[18−23] and intramolecular atomic rearrangements[24−27] have been activated on individual molecules using the STM. Working at low temperatures, transient intermediate states have also been resolved.[28] Chemical reactions can be stimulated by the STM electronically with the tunneling current, through the applied electric field between tip and sample or by a combination of both mechanisms. The tunneling electrons excite molecular states that participate in the formation of chemical bonds or activate vibrational modes and, thus, produce molecular changes associated with chemical reactions.[7−11,15,20,24] The electric field confined between the tip apex and the substrate has been shown to stimulate conformational transitions,[18,19] complex movements of molecules,[25−27] or to trigger dissociation reactions.[16,17] Additionally, it was shown recently in a STM-break junction setup that the electric field can be used to obtain a catalytic-like effect for the acceleration of a Diels−Alder

Received: January 27, 2017
Accepted: April 24, 2017
Published: April 24, 2017

DOI: 10.1021/acsnano.7b00612
ACS Nano 2017, 11, 4703−4709

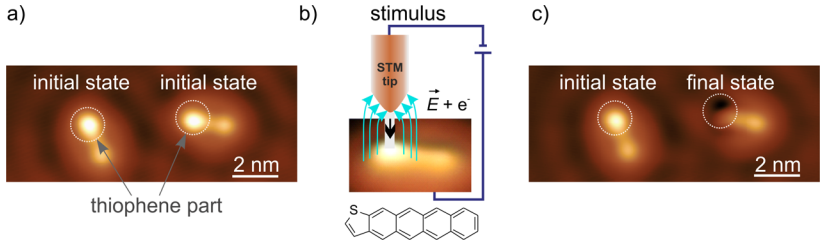

Figure 1. STM investigation of the desulfurization reaction on single TCT molecules adsorbed on Cu(111). (a) STM topographic image (I = 100 pA, V = 100 mV) before the reaction showing two TCT molecules in initial conformation 1. (b) Schematic representation of the STM-induced desulfurization reaction on a single molecule initiated by the electric field $\vec{E}$ (the field lines are symbolized by the cyan arrows) and the tunneling electrons e^- (the current flow is symbolized by the black arrow). Bottom panel: chemical structure of the TCT molecule. (c) STM image after the reaction was induced in the molecule at the right part of panel (a). This molecule is now in the final conformation 2. The white circles indicate the thiophene group of the molecule before and after the reaction.

reaction,[29] which highlights the potential of oriented electric fields to control chemical processes.[30]

In our study, the electric field is employed to trigger locally a desulfurization process on a single molecular subunit, a thiophene ring, part of a tetracenothiophene (TCT) molecule. The spatial mapping of the molecular states close to the Fermi energy of the substrate, complemented with density functional theory (DFT) calculations, enables us to identify the two elementary steps of the direct desulfurization reaction, *i.e.*, the successive cleavage of the two C−S bonds.

RESULTS AND DISCUSSION

To address locally the thiophene moiety of the TCT molecules (chemical structure in Figure 1b), a submonolayer amount of TCT was deposited on the closed-packed copper Cu(111) surface held at 200 K. At lower temperatures (6 K), individual molecules are imaged by the STM as asymmetric "dumbbell"-shaped protrusions (Figure 1a). The thiophene unit appears brighter, showing a higher density of states compared to the tetracene part (for a detailed structural analysis see the Supporting Information (SI), adsorption conformation). The desulfurization reaction is activated by precisely positioning the STM tip apex on top of the thiophene ring and applying as stimulus a short voltage pulse that creates a strong electric field in the junction and injects electrons into the system (Figure 1b). Each step of the chemical reaction sequence is imaged by STM with noninvasive tunneling parameters that do not affect the molecular configuration. Two irreversible reaction pathways, differing by the action of the applied stimulus, are successfully activated locally converting single molecules from the initial state **1** to the final state **2** (Figure 1a,c).

One pathway, which we call **R**, leads to a direct transition from the initial state **1** to the final state **2**. For the second pathway we can follow a two-step reaction, where we call the individual steps **RI** and **RII**. The end-products of **RI** + **RII** and of **R** are equivalent as demonstrated in Figure 2, and thus **R** = **RI** + **RII**, as we will show in detail later. Placing the tip above the thiophene ring of **1** (Figure 2a) at a large relative tip−molecule distance of 2−3 nm and applying a voltage above 5.5 V to the sample, an intermediate state **1i** is reached. The definition of the relative tip−molecule distance is described in the Methods section. The induced reaction results in changes of the molecular structure corresponding to a reduced density of states at the thiophene site and, in addition, to the appearance of a dark spot at the initial position of the sulfur atom (Figure 2a, central panel). For the second step **RII**, the relative distance between the tip and the thiophene ring was reduced to values

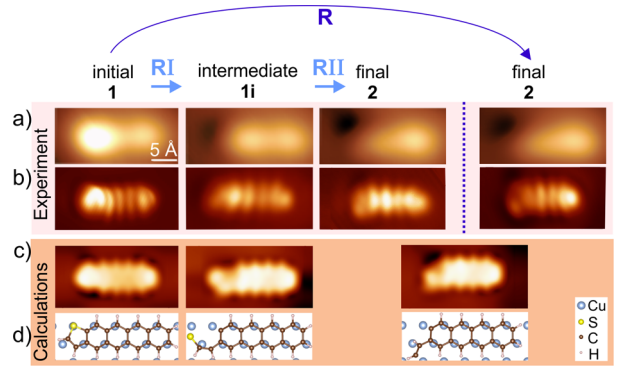

Figure 2. Molecular conformations at each stage of the direct desulfurization reaction obtained by STM investigations and DFT calculations. (a) Topographic images acquired in constant current mode. The reaction R represents the reaction that directly transforms the system from state 1 to the final state 2. The reactions RI and RII represent the two steps of the desulfurization process, from the initial state 1 to the intermediate state 1i and from 1i to the final state 2. (b) Spatial maps of the molecular states obtained with a functionalized tip, acquired in constant height mode (I = 100 pA, V = −1 V left image, I = 100 pA, V = 100 mV all other images). (c) Molecular appearances in the Tersoff−Hamann approximation obtained from DFT-vdW simulations for each molecular state. (d) Ball-and-stick representation of the calculated molecular sequences on the Cu(111) surface (top views).

smaller than 1.25 nm while applying a voltage pulse between 1.5 and 4.5 V, depending on the distance. Again, a drastic change is observed in the topographic appearance at the reacted side of the molecules, where the density of states is further reduced. The images in Figure 2a are acquired with a metal tip that does not allow resolving the molecular orbitals.

A comparison between STM images taken with a functionalized tip showing the orbital structure of the molecules and DFT calculations using van der Waals density functional in which exchange and correlations are described consistently (vdW-DF-cx)[31,32] reveals the detailed reaction pathway of the desulfurization reaction mechanism. Figure 2b shows the spatial mapping of the molecular state located at the Fermi energy of the reactant, intermediate, and product of this two-step reaction. These images are acquired in constant height mode using a functionalized molecular tip. The functionalization is performed by standard vertical manipulation to place a TCT molecule at the tip apex. The initial configuration 1 (Figure 2b, left panel) resembles the lowest unoccupied molecular orbital in the gas phase, gas-phase LUMO, of TCT (see SI, electronic

DOI: 10.1021/acsnano.7b00612
ACS Nano 2017, 11, 4703−4709

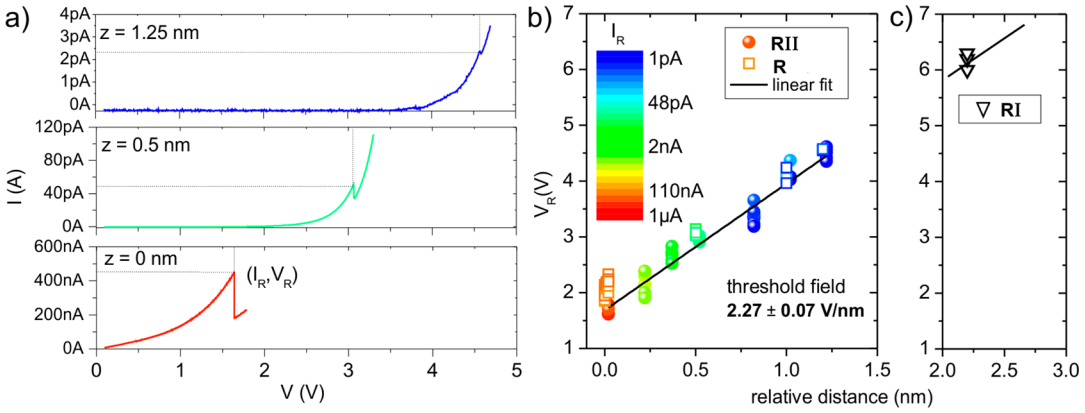

Figure 3. Experimental evidence for the electric-field-stimulated reaction. (a) $I(V)$ curves recorded at relative distances z from the height where the feedback loop was switched off and approached by 200 pm. The origin of the z axis corresponds to a tunneling resistance of 16.5 ± 1.2 MΩ. The sudden change in the current traces at which the reaction occurs is marked by (I_R,V_R). (b) The threshold voltage V_R at which the reaction pathways R (1-2 transition) and RII (1i-2 transition) are activated, respectively, follows a linear dependence with z, a behavior which is characteristic of an electric-field-driven reaction. The threshold current, I_R, is depicted in the color map. (c) At larger tip−sample distances, with the tip withdrawn by more than 2 nm, the electric field stimulates the pathway RI (1-1i transition) only. The current at these large tip−sample distances is of the order of the noise level of 0.1 pA.

structure) and is comparable to the calculated STM appearance obtained within the Tersoff−Hamann approximation (Figure 2c, left panel).[33] This observation is traced back to a strong hybridization at the interface and to a charge transfer from the substrate to the molecule, a process which shifts the energy of this orbital, named here surface-modified LUMO, toward the Fermi level, similar to the behavior of the chemical analogue anthradithiophene when adsorbed on Cu(111).[34] The simulated STM images are in qualitative agreement with the experimental topographies (Figure 2b,c, center and right panels). In the STM images, the intermediate, **1i**, and final, **2**, conformations appear with a depression in close vicinity of the molecule (Figure 2a,b, center and right panels). This feature is reproduced by the calculations and is in the location of the former S position in the intermediate state **1i** and the final state **2**. The calculated molecular structures, plotted in a ball-and-stick representation in Figure 2d, provide snapshots of the atomic structure of the molecules-substrate system along the reaction pathway. Based on these experimental and theoretical evidences, we exclude conformational changes related to lateral translation or the scission of other chemical bonds, as described in detail in the SI.

The analysis reveals that the **RI** reaction consists of the scission of one of the two carbon−sulfur bonds, opening the thiophene ring (Figure 2d). The cleaved bond results in a geometric reorganization of the two carbon atoms of the thiophene ring, increasing angles between C−C bonds, which leads to the accommodation of the sulfur atom at a new position. When the second carbon−sulfur bond is dissociated in **RII**, the system releases energy, and, thus, the sulfur is repelled from the surrounding of the molecule. This step is accompanied by further repositioning of the two carbon atoms. Therefore, the entire process encompasses cleavage of the C−S bonds, new bond formations between the opened thiophene ring and the surface, distortions, and translation of the S atom.

Next, we discuss the experimental procedure used to deduce the nature of the stimuli which trigger the desulfurization reaction. At large tip−sample distances the dominating stimulus is the electric field present in the tunneling junction when a bias voltage is applied. By decreasing the tip−sample distance, the tunneling current increases, and, thus, more electrons are injected into the system. In our analysis we have been able to correlate the two reaction steps **RI** and **RII** with two different regimes. To trigger and to track the reaction **RI**, we performed detailed studies of the experimental parameters required to initiate the reaction. We first acquired a topographic image of the molecule in state **1** and then stabilized the tip above the thiophene moiety at the tunneling parameters I = 100 pA and U = 100 mV. After disabling the feedback loop that controls the tip height, we increased the tip-molecule distance z to about 2.2 nm (z = 0 corresponds to a tunnel resistance of 16.5 ± 1.2 MΩ) and applied a short voltage pulse of 5 V (minimum duration 100 μs). At these large tip−sample distances, the current was in the noise limit of our current amplifier. This observation leads us to conclude that the dominant stimulus of **RI** is the electric field. It transforms the system from the initial to the intermediate state. The successful transition to the intermediate state **1i** is confirmed afterward by topographic imaging.

The second step **RII** can only be activated at much shorter distances between tip and thiophene ring. To trigger **RII**, we placed the STM tip on top of the thiophene unit at a distance stabilized by the tunneling parameters (I = 100 pA, U = 100 mV), and we switched the feedback loop off. Subsequently, we measured at various tip−sample distances z (between 0 and 1.25 nm relative distances) the transitions **RII** (**1i-2** path) that we could detect in the voltage-dependent current traces by recording $I(V)$ curves (Figure 3a). At these distances we have a measurable current, and we can detect a sudden decrease of the current as a step-like feature in the $I(V)$ traces. This step-like feature coincides with a change in the local density of states at the submolecular level. This abrupt change indicates the transition from state **1i** to the final state **2**, as identified subsequently in the STM images. The current and the voltage values for which the reaction is stimulated are marked with (I_R,V_R). The voltages V_R which trigger the pathway **RII** follow a linear dependence with z (Figure 3b solid circles). This is a characteristic behavior of an electric-field-driven reaction.[18,19] The slope of this linear dependence is about 2 V nm^{-1} and represents the critical electric field necessary to trigger the reaction. Hence, the electric field is the stimulus that activates

DOI: 10.1021/acsnano.7b00612
ACS Nano 2017, 11, 4703−4709

the pathway **RII**, but the necessity to work at short tip-thiophene distances to run this reaction step ensures the injection of electrons into the molecular system (see Figure 3b). In Figure 3c the (I_R,V_R) values at which reaction **R1** is activated are plotted. It is observed that these values follow exactly the linear dependence extracted in Figure 3b. If we work in the regime of short tip−sample distances, we can directly transform the system from the initial state **1** to the final state **2** (pathway **R**), since we apply at the same time a sufficiently high electric field and inject a sufficiently high amount of electrons into the system to break both C−S bonds. On the time scale of the measurement, we cannot observe the intermediate product. We observe exactly the same end-product for **RI** + **RII** that we observe for **R** (see Figure 2). When a functionalized tip was used (Figure 2b), the molecules in the final state have the same molecular orbital shape, especially at the reacted side of the molecule, although the relative intensities of different images vary slightly due to different conformations of the molecule attached to the tip apex. In addition, the corresponding (I_R,V_R) values are very similar to the values obtained for **RII** (open squares in Figure 3b). On the basis of these arguments we conclude that **R** = **RI** + **RII**.

Therefore, a critical field of about 2 V nm^{-1} has to be overcome to activate the reaction pathways, **RI** and **RII**. A key difference between the reaction paths lies in the activation mechanism. From the analysis, we conclude that **RI** is triggered only by the electric field, whereas **RII** is driven by a combination of the electric field and the injection of electrons. The direct desulfurization reaction, including all pathways, can be activated only with a positive voltage polarity, highlighting the importance of the electric field.

The adsorption of thiophene, or other molecules containing the thiophene moiety, on different metallic surfaces is known to cause a reduction of the activation barrier for the desulfurization reaction, which has been shown to be thermally stimulated at room temperature and above.[35−37] In our case, the adsorption of tetracenothiophene on Cu(111) also lowers this activation barrier. Here, we have demonstrated the use of an electric field as stimulus at cryogenic temperatures to overcome the remaining barrier for the direct desulfurization reaction.

The first step **RI** is triggered by the electric field oriented from the sample toward the tip, practically in the absence of tunneling electrons. The induced electron density of the adsorbed molecule in the initial state **1** (Figure 4a) shows an electron transfer from the surface to the entire molecule that corresponds approximately to one additional electron populating the LUMO of the adsorbed molecule, *i.e.*, essentially a TCT anion. This surface-modified LUMO, shown in Figure 4b, does not show typical bonding character with respect to the C−S−C bonds, as it is reflected in the absence of electronic charge at the position of the S atom. The interaction with the applied electric field disturbs this arrangement in the vicinity of the tip position and may lower the energy barrier of the reaction. In addition, it acts on the C−S dipole of the TCT anion while leading to a weakening of the sulfur−carbon bond. According to a Bader charge analysis,[38−40] the positive charge on the S atom is +0.2 e, and the negative charges on the two neighboring C atoms are −0.29 e and −0.16 e. The positively charged S atom is attracted toward the tip, while the two negatively charged neighboring C atoms are repelled under the applied electric field, leading to an elongation of the C−S bonds and, eventually, to the breakdown of one of them. The exact process

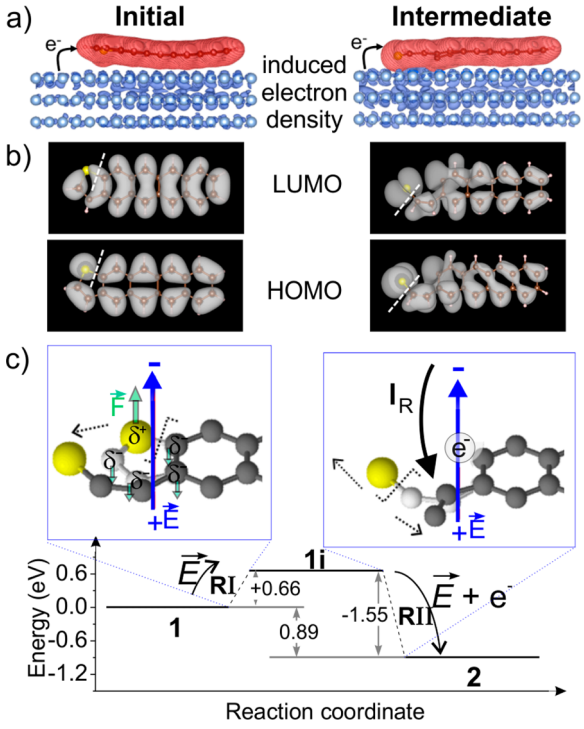

Figure 4. Effect of the electric field on the reaction mechanism. (a) Induced electron density, ρ_{ind}, in the initial (left panel) and intermediate states (right panel) calculated as $\rho_{ind} = \rho_{total} - \rho_{mol} - \rho_{surf}$ with ρ_{total} the charge density of the entire system, ρ_{mol} the charge density of the molecule and ρ_{surf} the charge density of the clean surface slab. Isovalues are 2×10^{-2} e/bohr^3 and -2×10^{-4} e/bohr^3, respectively, displayed in red and blue. (b) Surface-modified LUMO and HOMO of the initial (left panels) and intermediate states (right panels). (c) Energetic pathway of the desulfurization reaction considering the total energy of each molecular conformation with respect to the initial state. In the final state, the expelled S atom is considered adsorbed in its equilibrium site on Cu(111) without interaction with the TCT molecular part. Insets: Ball-and-stick representation superposing the molecular structures at the thiophene side before (light-gray) and after (dark-gray) the reaction RI, left panel, and RII, right panel, respectively. The bond cleavage and the modifications of the position are drawn with dotted lines. The electric field and the tunneling current are schematized as a colored arrow (blue) and solid-black arrow, respectively. The charge distribution of the initial state and the forces acting on the system due to the presence of the electric field are indicated by green arrows.

might be similar to the breaking of a C−S bond in a nonradiative decay of excited thiophenes.[41]

The corresponding energies of the initial, intermediate, and final states are shown in Figure 4c. An energy barrier for **RI** of about 0.9 eV has been estimated using an improved nudged elastic band minimization (NEB) method called the climbing image method.[42,43] Indeed, this finding is consistent with DFT calculations reporting modifications of C−S bonds under electric fields[44] and experimental evidence of processes induced by an electric field.[16−19,25−27]

The second reaction step **RII** is also driven with the same bias polarity. However, as already mentioned, it occurs only if both the electric field and the injection of electrons are present. Thus, the reaction is triggered by a combination of electronic excitations and electric field effects. The electric field with the correct polarity induces changes of the local charge distribution and modifies the energy barrier of the reaction, as in reaction

DOI: 10.1021/acsnano.7b00612
ACS Nano 2017, 11, 4703−4709

RI. Additionally, the injection of electrons increases the population of the molecular orbital visualized at the Fermi level of the metal (Figure 2b). This orbital has clear antibonding character (Figure 4a,b) and, therefore, increases the reaction rate for the scission of the remaining C−S bond and the removal of the S atom. Alternatively, the injected electrons might couple to vibronic states of the molecule which consequently could cleave the remaining C−S bond. This reaction is exothermic by about 0.89 eV (Figure 4c), which means that the sulfur atom has sufficient energy, compared to diffusion barriers of about 0.25 eV for S/Cu(111),[45] to diffuse on the surface before reaching its equilibrium adsorption state on the Cu surface.

CONCLUSION

Our investigations reveal the two-step chemical pathway of the direct desulfurization of tetracenothiophene molecules adsorbed on a Cu(111) surface. The dissociation reaction is triggered locally by an electric field applied to the confined tunnel junction between the STM tip and the thiophene unit. Experimental control at the atomic level and comparison with theoretical calculations resolve the two elementary steps of this direct desulfurization reaction. The detailed experimental analysis of the stimuli involved to initiate the chemical reaction suggests that the first step, dissociation of one of the two C−S bonds, is activated solely by the electric field, whereas the second step, the breaking of the remaining C−S bond, is a consequence of the two driving forces electric field and injection of electrons. Triggering chemical processes by applying an electric field to a specific molecular moiety highlights the high potential of oriented external electric fields for single-molecule chemistry.[30]

METHODS

Synthesis. Tetraceno[2,3-*b*]thiophene (TCT) was synthesized from tetraceno[2,3-*b*]thiophene-5,12-dione.[46] First, thiophene-2,3-dicarbaldehyde was obtained from thiophene-3-carbaldehyde (0.98 g, 7 mmol) and then condensed with 1,4-dihydroxyanthracene (1.46 g, 7 mmol), obtained from 1,4-anthracenedione, to yield the corresponding tetracenothiophene quinone. The aldol condensation reaction was conducted in a mixture of ethanol and tetrahydrofuran using 15% aqueous solution of sodium hydroxide as a base. The quinone (1.0 g, 3.18 mmol) was then reduced to tetraceno[2,3-*b*]thiophene using sodium borohydride ($NaBH_4$, 1.2 g, 31.85 mmol, 10 equiv) in anhydrous tetrahydrofuran (60 mL) for the reduction to the diol, followed by deoxygenation with tin(II)chloride ($SnCl_2$, 3.59 g, 15.9 mmol, 5 equiv)/10% aqueous solution of HCl. Finally, tetraceno[2,3-*b*]thiophene was purified by sublimation.

Experimental Details. The experiments were performed under ultrahigh-vacuum (UHV) conditions. The Cu(111) substrate was cleaned by standard procedures of Ar+ ion bombardment and subsequent annealing at 800 K. The TCT molecules were thermally sublimated from a ceramic crucible at 485 K onto the Cu(111) surface held at 200−250 K during the deposition. Subsequently, the sample was transferred *in situ* into the STM operating at low temperature (6 K). The STM measurements were carried out by applying the bias voltages to the sample in both constant-current and constant-height modes. Submolecular resolution imaging was achieved by placing a TCT molecule at the apex of the tip in a vertical manipulation procedure. The relative tip−sample distance is referred to the following set point. The STM tip was stabilized at 100 pA, 100 mV above the thiophene ring of the molecules in the initial state **1**. Then, the feedback loop was switched off, and the tip was approached toward the surface by 200 pm. The tunneling resistance at this position is 16.5 ± 1.2 MΩ. This new tip−sample distance was defined as the origin of our *z*-axis.

Computational Details. DFT-vdW calculations were performed using the VASP code.[47,48] To model the TCT/Cu(111) system, a 4 layer slab 8 × 6 periodic supercell was employed. Ion−electron interaction was described with the projector augmented-wave (PAW) method,[49] and exchange−correlation was modeled within the generalized gradient approximation (GGA).[50] The van der Waals dispersion forces were included using the vdW-DF-cx method.[31,32] We considered a 500 eV energy cutoff in the plane wave expansion, with a 2 × 3 k-point mesh in the 1 × 1 unit cell as sampling of the Brillouin zone reciprocal space. Electronic convergence criterion was 1×10^{-4} for all static calculations, and convergence on forces in the relaxations was 0.05 eV/Å. STM appearance simulations were computed in the Tersoff−Hamann approximation.[33]

ASSOCIATED CONTENT

Supporting Information

The Supporting Information is available free of charge on the ACS Publications website at DOI: 10.1021/acsnano.7b00612.

A detailed description of the adsorption conformation of TCT molecules on Cu(111) is included in the supporting file (PDF)

AUTHOR INFORMATION

Corresponding Authors

*E-mail: bogdana.borca@infim.ro.
*E-mail: u.schlickum@fkf.mpg.de.

ORCID

Bogdana Borca: 0000-0001-5485-4536
Rémi Pétuya: 0000-0002-3118-6966
Peter Wahl: 0000-0002-8635-1519

Present Addresses

▽Institut des Sciences Analytiques et de Physico-Chimie pour l'Environnement et les Matériaux (IPREM) UMR 5254, 64053 Pau, France
○Karlsruher Institut für Technologie (KIT), Engesserstrasse 13, 76131 Karlsruhe, Germany
◆Stanford University, Stanford, California 94305, United States

Author Contributions

¶These authors contributed equally.

Notes

The authors declare no competing financial interest.

ACKNOWLEDGMENTS

We acknowledge funding by the Emmy-Noether-Program of the Deutsche Forschungsgemeinschaft and the SFB 767. R.P. and A.A. thank the Basque Departamento de Universidades e Investigación (grant no. IT-756-13) and the Spanish Ministerio de Economía y Competitividad (grant nos. FIS2013-48286-C2-8752-P and FIS2016-75862-P) for financial support. The authors thank M. Ternes for fruitful discussions.

REFERENCES

(1) Falkowski, P. G.; Fenchel, T.; Delong, E. F. The Microbial Engines That Drive Earth's Biogeochemical Cycles. *Science* **2008**, *320*, 1034−1038.
(2) Wortmann, U. G.; Paytan, A. Rapid Variability of Seawater Chemistry. *Science* **2012**, *337*, 334−336.
(3) Zhelezinskaia, I.; Kaufman, A. J.; Farquhar, J.; Cliff, J. Large Sulfur Isotope Fractionations Associated with Neoarchean Microbial Sulfate Reduction. *Science* **2014**, *346*, 742−744.

DOI: 10.1021/acsnano.7b00612
ACS Nano 2017, 11, 4703−4709

(4) Babich, I. V.; Moulijn, J. A. Science and Technology of Novel Processes for Deep Desulfurization of Oil Refinery Streams: a Review. *Fuel* **2003**, *82*, 607−631.
(5) Topsøe, H.; Clausen, B. S.; Massoth, F. E. *Catalysis Science and Technology*; Anderson, J. R., Boudart, M., Eds.; Springer-Verlag: New York, 1996; Vol. *11*, pp 1−269.
(6) Gary, J. H.; Handwerk, G. E.; Kaiser, M. J. *Petroleum Refining: Technology and Economics, Fifth ed.*; CRC Press: Boca Raton, FL, 2007.
(7) Lee, H. J.; Ho, W. Single-Bond Formation and Characterization with a Scanning Tunneling Microscope. *Science* **1999**, *286*, 1719−1722.
(8) Hla, S.-W.; Bartels, L.; Meyer, G.; Rieder, K.-H. Inducing All Steps of a Chemical Reaction with the Scanning Tunneling Microscope Tip: Towards Single Molecule Engineering. *Phys. Rev. Lett.* **2000**, *85*, 2777−2780.
(9) Ohmann, R.; Vitali, L.; Kern, K. Actuated Transitory Metal - Ligand Bond as Tunable Electromechanical Switch. *Nano Lett.* **2010**, *10*, 2995−3000.
(10) Mohn, F.; Repp, J.; Gross, L.; Meyer, G.; Dyer, M. S.; Persson, M. Reversible Bond Formation in a Gold-Atom-Organic-Molecule Complex as a Molecular Switch. *Phys. Rev. Lett.* **2010**, *105*, 266102−266105.
(11) Liljeroth, P.; Repp, J.; Meyer, G. Current-Induced Hydrogen Tautomerization and Conductance Switching of Naphthalocyanine Molecules. *Science* **2007**, *317*, 1203−1206.
(12) Simic-Milosevic, V.; Mehlhorn, M.; Rieder, K.-H.; Meyer, J.; Morgenstern, K. Electron Induced Ortho-Meta Isomerization of Single Molecules. *Phys. Rev. Lett.* **2007**, *98*, 116102−1−4.
(13) Maksymovych, P.; Sorescu, D. C.; Jordan, K. D.; Yates, J. T., Jr. Collective Reactivity of Molecular Chains Self-Assembled on a Surface. *Science* **2008**, *322*, 1664−1667.
(14) Néel, N.; Lattelais, M.; Bocquet, M.-L.; Kröger, J. Depopulation of Single-Phthalocyanine Molecular Orbitals upon Pyrrolic-Hydrogen Abstraction on Graphene. *ACS Nano* **2016**, *10*, 2010−2016.
(15) Shen, T. C.; Wang, C.; Abeln, G. C.; Tucker, J. R.; et al. Atomic-Scale Desorption Through Electronic and Vibrational Excitation Mechanisms. *Science* **1995**, *268*, 1590−1592.
(16) Serrate, D.; Moro-Lagares, M.; Piantek, M.; Pascual, J. I.; Ibarra, M. R. Enhanced Hydrogen Dissociation by Individual Co Atoms Supported on Ag(111). *J. Phys. Chem. C* **2014**, *118*, 5827−5832.
(17) Minato, T.; Kajita, S.; Pang, C. L.; Asao, N.; Yamamoto, Y.; Nakayama, T.; Kawai, M.; Kim, Y. Tunneling Desorption of Single Hydrogen on the Surface of Titanium Dioxide. *ACS Nano* **2015**, *9*, 6837−6842.
(18) Qiu, X. H.; Nazin, G. V.; Ho, W. Mechanisms of Reversible Conformational Transitions in a Single Molecule. *Phys. Rev. Lett.* **2004**, *93*, 196806−1−4.
(19) Alemani, M.; Peters, M. V.; Hecht, S.; Rieder, K.-H.; Moresco, F.; Grill, L. Electric Field Induced Isomerization of Azobenzene by STM. *J. Am. Chem. Soc.* **2006**, *128*, 14446−14447.
(20) Lastapis, M.; Martin, M.; Riedel, D.; Hellner, L.; Comtet, G.; Dujardin, G. Picometer-Scale Electronic Control of Molecular Dynamics Inside a Single Molecule. *Science* **2005**, *308*, 1000−1003.
(21) Iancu, V.; Deshpande, A.; Hla, S.-W. Manipulating Kondo Temperature *via* Single Molecule Switching. *Nano Lett.* **2006**, *6*, 820−823.
(22) Henningsen, N.; Franke, K. J.; Torrente, I. F.; Schulze, G.; Priewisch, B.; Ruck-Braun, K.; Dokic, J.; Klamroth, T.; Saalfrank, P.; Pascual, J. I. Inducing the Rotation of a Single Phenyl Ring with Tunneling Electrons. *J. Phys. Chem. C* **2007**, *111*, 14843−14848.
(23) Simic-Milosevic, V.; Morgenstern, K. Bending a Bond within an Individual Adsorbed Molecule. *J. Am. Chem. Soc.* **2009**, *131*, 416−417.
(24) Wang, Y.; Kröger, J.; Berndt, R.; Hofer, W. A. Pushing and Pulling a Sn Ion through an Adsorbed Phthalocyanine Molecule. *J. Am. Chem. Soc.* **2009**, *131*, 3639−3643.
(25) Grill, L.; Rieder, K.-H.; Moresco, F.; et al. Exploring the Interatomic Forces between Tip and Single Molecules during STM Manipulation. *Nano Lett.* **2006**, *6*, 2685−2689.
(26) Grill, L.; Rieder, K.-H.; Moresco, F.; Rapenne, G.; Stojkovic, S.; Bouju, X.; Joachim, C. Rolling a Single Molecular Wheel at the Atomic Scale. *Nat. Nanotechnol.* **2007**, *2*, 95−98.
(27) Kudernac, T.; Ruangsupapichat, N.; Parschau, M.; Maciá, B.; Katsonis, N.; Harutyunyan, S. R.; Ernst, K.-H.; Feringa, B. L. Electrically Driven Directional Motion of a Four-Wheeled Molecule on a Metal Surface. *Nature* **2011**, *479*, 208−211.
(28) Pavliček, N.; Schuler, B.; Collazos, S.; Moll, N.; Pérez, D.; Guitián, E.; Meyer, G.; Peña, D.; Gross, L. On-Surface Generation and Imaging of Arynes by Atomic Force Microscopy. *Nat. Chem.* **2015**, *7*, 623−628.
(29) Aragonès, A. C.; Haworth, N. L.; Darwish, N.; Ciampi, S.; Bloomfield, N. J.; Wallace, G. G.; Diez-Perez, I.; Coote, M. L. Electrostatic Catalysis of a Diels−Alder Reaction. *Nature* **2016**, *531*, 88−91.
(30) Shaik, S.; Mandal, D.; Ramanan, R. Oriented Electric Fields as Future Smart Reagents in Chemistry. *Nat. Chem.* **2016**, *8*, 1091−1098.
(31) Berland, K.; Hylgaard, P. Exchange Functional that Tests the Robustness of the Plasmon Description of the van der Waals Density Functionals. *Phys. Rev. B: Condens. Matter Mater. Phys.* **2014**, *89*, 035412.
(32) Björkman, T. Testing Several Recent van der Waals Density Functionals for Layered Structures. *J. Chem. Phys.* **2014**, *141*, 074708−1−6.
(33) Tersoff, J.; Hamann, D. R. Theory and Application for the Scanning Tunneling Microscope. *Phys. Rev. Lett.* **1983**, *50*, 1998−2001.
(34) Borca, B.; Schendel, V.; Pétuya, R.; Pentegov, I.; Michnowicz, T.; Kraft, U.; Klauk, H.; Arnau, A.; Wahl, P.; Schlickum, U.; Kern, K. Bipolar Conductance Switching of Single Anthradithiophene Molecules. *ACS Nano* **2015**, *9*, 12506−12512.
(35) Stöhr, J.; Gland, J. L.; Kollin, E. B.; Koestner, R. J.; Johnson, A. L.; Muetterties, E. L.; Sette, F. Desulfurization and Structural Transformation of Thiophene on the Pt (111) Surface. *Phys. Rev. Lett.* **1984**, *53*, 2161−2164.
(36) Dinca, L. E.; MacLeod, J. M.; Lipton-Duffin, J.; Fu, C.; Ma, D.; Perepichka, D. F.; Rosei, F. Tailoring the Reaction Path in the On-Surface Chemistry of Thienoacenes. *J. Phys. Chem. C* **2015**, *119*, 22432−22438.
(37) Dinca, L. E.; Fu, C.; MacLeod, J. M.; Lipton-Duffin, J.; Brusso, J. L.; Szakacs, C. E.; Ma, D.; Perepichka, D. F.; Rosei, F. Unprecedented Transformation of Tetrathienoanthracene into Pentacene on Ni(111). *ACS Nano* **2013**, *7*, 1652−1657.
(38) Henkelman, G.; Arnaldsson, A.; Jónsson, H. A. Fast and Robust Algorithm for Bader Decomposition of Charge Density. *Comput. Mater. Sci.* **2006**, *36*, 354−360.
(39) Sanville, E.; Kenny, S. D.; Smith, R.; Henkelman, G. An Improved Grid-Based Algorithm for Bader Charge Allocation. *J. Comput. Chem.* **2007**, *28*, 899−908.
(40) Tang, W.; Sanville, E.; Henkelman, G. A. Grid-Based Bader Analysis Algorithm without Lattice Bias. *J. Phys.: Condens. Matter* **2009**, *21*, 084204−1−7.
(41) Salzmann, S.; Kleinschmidt, M.; Tatchen, J.; Weinkauf, R.; Marian, C. M. Excited States of Thiophene: Ring Opening as Deactivation Mechanism. *Phys. Chem. Chem. Phys.* **2008**, *10*, 380−392.
(42) Henkelman, G.; Uberuaga, B. P.; Jónsson, H. A. Climbing Image Nudged Elastic Band Method for Finding Saddle Points and Minimum Energy Paths. *J. Chem. Phys.* **2000**, *113*, 9901−9904.
(43) Henkelman, G.; Jónsson, H. Improved Tangent Estimate in the Nudged Elastic Band Method for Finding Minimum Energy Paths and Saddle Points. *J. Chem. Phys.* **2000**, *113*, 9978−9985.
(44) Ye, Y.; Zhang, M.; Liu, H.; Liu, X.; Zhao, J. Theoretical Investigation on the Oligothienoacenes under the Influence of External Electric Field. *J. Phys. Chem. Solids* **2008**, *69*, 2615−2621.
(45) Barth, J. V. Transport of Adsorbates at Metal Surfaces: from Thermal Migration to Hot Precursors. *Surf. Sci. Rep.* **2000**, *40*, 75−149.
(46) Kraft, U.; Anthony, J. E.; Ripaud, E.; Loth, M. A.; Weber, E.; Klauk, H. Low-Voltage Organic Transistors Based on Tetraceno[2,3-

DOI: 10.1021/acsnano.7b00612
ACS Nano 2017, 11, 4703−4709

b]thiophene: Contact Resistance and Air Stability. *Chem. Mater.* **2015**, *27*, 998−1004.
(47) Kresse, G.; Hafner, J. *Ab Initio* Molecular-Dynamics Simulation of the Liquid-Metal-Amorphous-Semiconductor Transition in Germanium. *Phys. Rev. B: Condens. Matter Mater. Phys.* **1994**, *49*, 14251−14269.
(48) Kresse, G.; Furthmuller, J. Efficient Iterative Schemes for *Ab Initio* Total-Energy Calculations Using a Plane-Wave Basis Set. *Phys. Rev. B: Condens. Matter Mater. Phys.* **1996**, *54*, 11169−11186.
(49) Blöchl, P. E. Projector Augmented-Wave Method. *Phys. Rev. B: Condens. Matter Mater. Phys.* **1994**, *50*, 17953−17979.
(50) Perdew, J. P.; Burke, K.; Ernzerhof, M. Generalized Gradient Approximation Made Simple. *Phys. Rev. Lett.* **1996**, *77*, 3865. Perdew, J. P.; Burke, K.; Ernzerhof, M. Generalized Gradient Approximation Made Simple [Phys. Rev. Lett. 77, 3865 (1996)]. *Phys. Rev. Lett.* **1997**, *78*, 1396−1396.

DOI: 10.1021/acsnano.7b00612
ACS Nano 2017, 11, 4703−4709

Electric-Field-Driven Direct Desulfurization

Supporting Information

Bogdana Borca,[1,2‡] Tomasz Michnowicz,[1‡] Rémi Pétuya,[3‡] Marcel Pristl,[1] Verena Schendel,[1] Ivan Pentegov,[1] Ulrike Kraft,[1] Hagen Klauk,[1] Peter Wahl,[1,4] Rico Gutzler,[1] Andrés Arnau,[3,5] Uta Schlickum [1] and Klaus Kern [1,6]

[1]Max Planck Institute for Solid State Research, 70569 Stuttgart, Germany,

[2]National Institute of Materials Physics, 077125 Măgurele-Ilfov, Romania,

[3]Donostia International Physics Centre, E-20018 Donostia - San Sebastián, Spain,

[4]SUPA, School of Physics and Astronomy, University of St Andrews, North Haugh, St Andrews, KY16 9SS, United Kingdom,

[5]Departamento de Física de Materiales UPV/EHU and Material Physics Center (MPC), Centro Mixto CSIC-UPV/EHU, E-20018 Donostia - San Sebastián, Spain,

[6]Institut de Physique, École Polytechnique Fédérale de Lausanne (EPFL), CH-1015 Lausanne, Switzerland.

Adsorption conformation

Tetracenothiophene (TCT) molecules and anthradithiophene (ADT) are structural analogs of pentacene, with one and two thiophene rings, respectively, at each molecular extremity as depicted in Figure S1a. When adsorbed on Cu(111) held at about 200 K, the molecules lie almost flat on the surface showing a “dumbbell”-like appearance in the STM images (Figure S1b). The height profiles along the molecules (Figure S1c) are acquired for the same tunneling conditions

(I = 100 pA, V = 100 mV). For pentacene, a symmetric line profile with two apparent elevations at both extremities is observed. The thiophene side in the TCT molecule appears brighter and, thus, it results in an asymmetric line profile with a higher apparent elevation on the thiophene part. ADT with its two thiophene rings appears again as symmetric "dumbbell"-like structure with two equally high elevations that are much high than the one of the pentacene molecule. This analysis allows us to clearly identify the thiophene position within the TCT molecules.

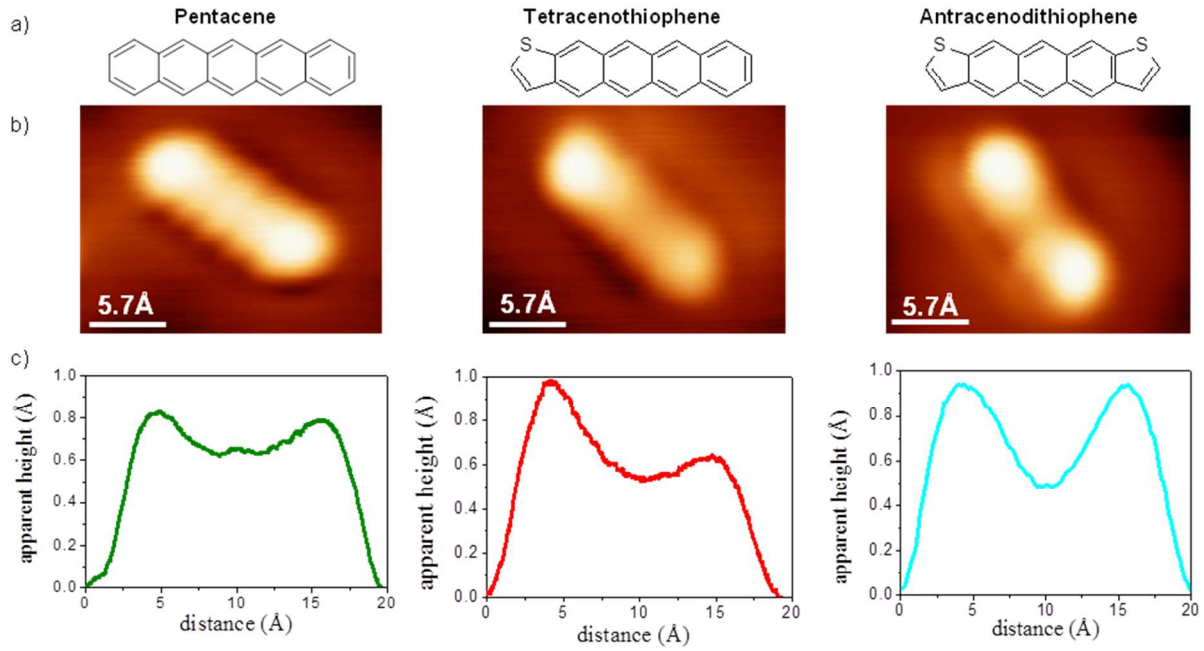

Figure S1. Adsorption of pentacene, TCT, and the ADT on Cu(111). a) Chemical sketch of each molecular structure. b) STM images acquired in constant current mode (I = 100 pA, V = 100 mV). c) Apparent height profiles along each molecule.

Desulfurization reaction

Here, we use a STM to induce and to investigate a direct desulfurization reaction of single TCT molecules adsorbed on the Cu(111) surface. The stimulus is a strong electric field confined at the tunneling junction. The reaction is triggered by positioning the STM tip apex above the

thiophene unit and applying a threshold electric field of approximatively 2 V/nm . In Figure S2a the STM topographic images acquired with a metal tip of the molecules before the reaction (state **1**) and after the desulfurization reaction (state **2**) are represented. The reaction implies the removal of the sulfur atom and the formation of a molecular derivative, covalently bonded to the surface. The apparent height of the molecules changes drastically at the thiophene side from the initial to the final state, but no change is revealed at the acene moiety (Figure S2b).

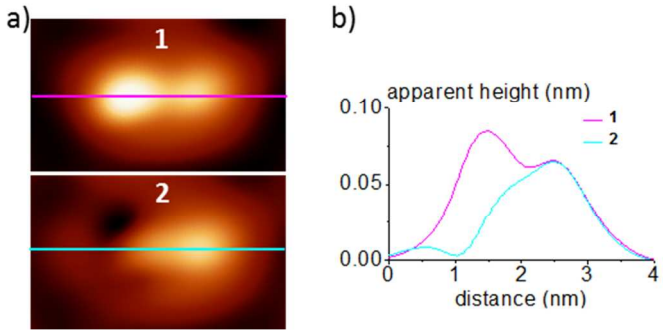

Figure S2. STM analysis of the desulfurization reaction. a) Topographic images (4 nm x 2.4 nm) acquired with a metallic tip (I = 100 pA, V = 100 mV) of TCT molecules before (state **1**) and after (state **2**) the desulfurization reaction. b) Line profiles, marked with the correspondent color in panel (a), showing the apparent height of the molecules in the initial and final state.

Electronic structure

In order to investigate TCT molecule adsorption on Cu(111), DFT-vdW calculations were performed varying the adsorption distance of the molecule with respect to the surface. For each calculation the geometry of the molecule was relaxed allowing the S atoms to move in (X, Y, Z) coordinates and the C and H atoms to move only in the plane defined by X and Y. The calculations reveal a broad and pronounced minimum at an adsorption distance z = 2.50 Å of the molecule above the surface (Figure S3a). Experimentally, only a single adsorption conformation

was found and, therefore, we performed a full relaxation of our minimal conformation allowing all molecular atoms to move in the X, Y, and Z coordinates. The projected density of states (PDOS) for the equilibrium conformation, obtained initially from the adsorption distance at 2.50 Å, is compared in Figure S3b with the PDOS for adsorption distances at 2.70 Å and 3.00 Å. The molecular state related to an adsorption distance of 2.50 Å shows a strong hybridization with the Cu(111) substrate. There is also a significant amount of charge transfer of about one electron to the lowest unoccupied molecular orbital (LUMO), which broadens and shifts the LUMO to lower energies, i. e., closer to the Fermi energy. Therefore, when imaged close to the Fermi level with a functionalized tip, the LUMO orbital of the TCT molecules becomes visible (Figure S3c,d).

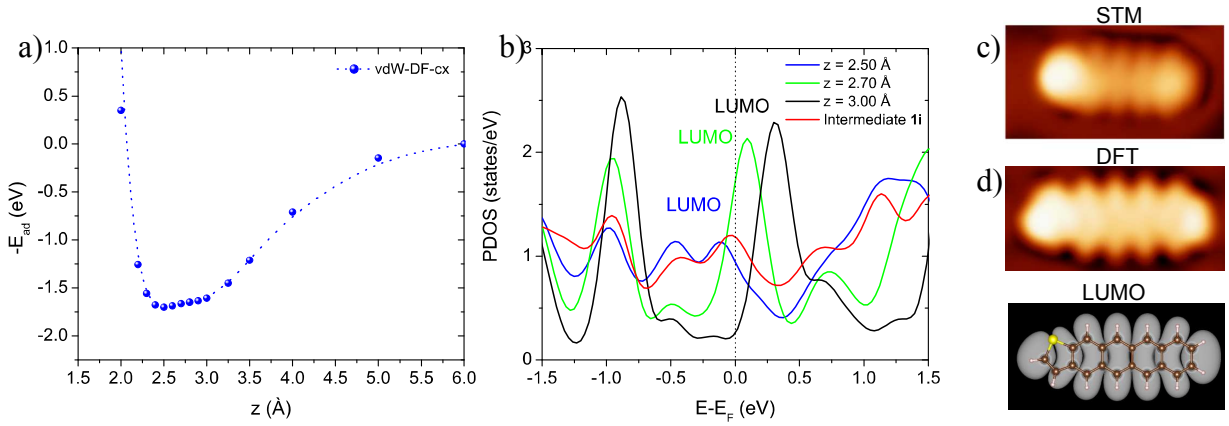

Figure S3. Electronic structure of TCT adsorbed on Cu(111). a) Adsorption energy ($-E_{ad}$) of the TCT as a function of the adsorption height *z* on Cu(111) from vdW-DF-cx calculations. b) PDOS calculated for the TCT initial state equilibrium geometry (z = 2.50 Å), at molecular adsorption distances of z = 2.70 and 3.00 Å, and for the intermediary reaction state **1i** shows a partial filling of the LUMO for decreasing distance *z*. c) STM image acquired with a functionalized tip resolving the orbital structure of TCT. d) Calculated molecular appearance of TCT on Cu(111) in the Tersoff-Hamann approximation and LUMO of the TCT free molecule in gas phase.

DFT calculations of the C-C bond scission.

To eliminate the possibility of a different interpretation of the experimental results, we performed DFT calculations considering the scission of the other bonds of the thiophene group. In Figure S4a and S4b the models for the dissociation of the C-C bonds are represented. These structures are single point energy calculations. Geometrical relaxations have been further performed for the left and middle structures from Figure S4, leading to the ring closure (the return to TCT geometry) or C-S bond breaking (giving a separated S-CH fragment), respectively. No geometrical relaxation has been performed for the structure in the right panel, but in the eventuality such relaxation would not lead to previously mentioned outcomes, a very different appearance from the experimental data is expected.

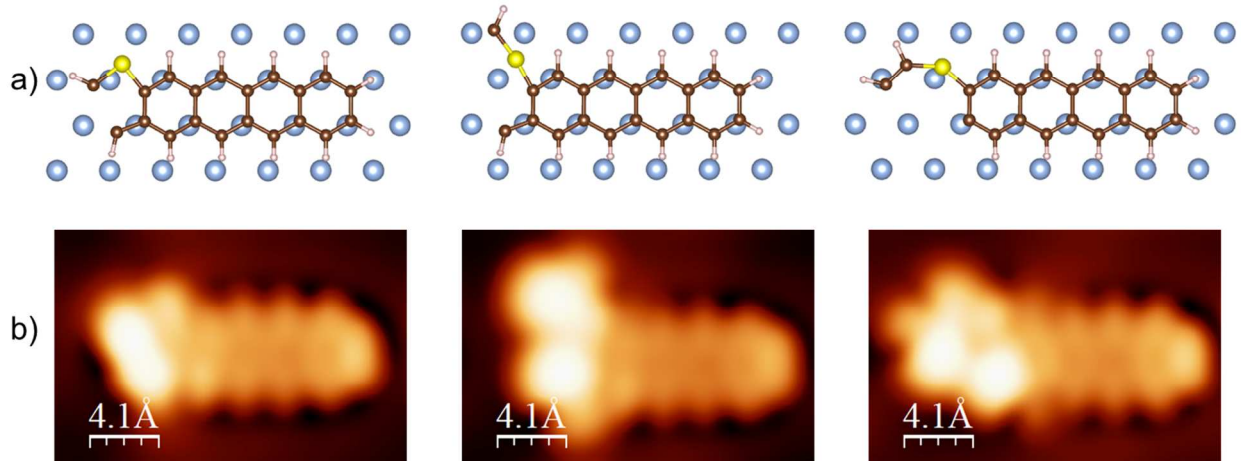

Figure S4. Calculated molecular appearances in the Tersoff-Hamann approximation considering different possibilities for the dissociation of the C-C bonds as represented in panel (a) in ball-and-stick models and in panel (b) in the simulated images.